

1

## 2 **Supplementary Information for**

### 3 **Learning complex models with invertible neural networks: a likelihood-free Bayesian** 4 **approach**

5 **Stefan T. Radev, Ulf K. Mertens, Andreas Voss, Lynton Ardizzone, and Ullrich Köthe**

6 **Stefan Radev.**

7 **E-mail: stefan.radev@psychologie.uni-heidelberg.de**

#### 8 **This PDF file includes:**

- 9     Supplementary text
- 10    Fig. S1
- 11    Captions for Movies S1 to S3
- 12    Captions for Databases S1 to S2
- 13    References for SI reference citations

#### 14 **Other supplementary materials for this manuscript include the following:**

- 15     Movies S1 to S3
- 16     Databases S1 to S2

## Supporting Information Text

Complete code for all examples used in this paper is available at <https://github.com/stefanradev93/cINN>.

## Performance metrics

In the following, the computation of the performance metrics used throughout the main text is detailed.

**Normalized Root Mean Squared Error.** The normalized root mean squared error (NRMSE) between a sample of true parameters  $\{\theta^{(i)}\}_{i=1}^n$  and a sample of estimated parameters  $\{\hat{\theta}^{(i)}\}_{i=1}^n$  is given by:

$$NRMSE = \sqrt{\sum_{i=1}^n \frac{(\theta^{(i)} - \hat{\theta}^{(i)})^2}{\theta_{max} - \theta_{min}}} \quad [1]$$

Due to the normalization factor  $\theta_{max} - \theta_{min}$ , the NRMSE is scale-independent, and thus suitable for comparing the recovery across parameters having different numerical ranges. The NRMSE is zero when the estimates are exactly equal to the true values.

**Coefficient of Determination .** The coefficient of determination  $R^2$  gives the proportion of variance in a sample of true parameters  $\{\theta^{(i)}\}_{i=1}^n$  that is "explained" by a sample of estimated parameters  $\{\hat{\theta}^{(i)}\}_{i=1}^n$ . It is computed as:

$$R^2 = 1 - \sum_{i=1}^n \frac{(\theta^{(i)} - \hat{\theta}^{(i)})^2}{(\theta^{(i)} - \bar{\theta})^2} \quad [2]$$

where  $\bar{\theta}$  denotes the mean of the true parameter samples. When  $R^2$  equals 1, it means that the estimates are perfect reconstructions of the true parameters.

**Kullback-Leibler Divergence.** The Kullback-Leibler divergence ( $D_{KL}$ ) quantifies the increase in entropy incurred by approximating a target probability distribution  $P$  with a distribution  $Q$ . Its general form for absolutely continuous distributions is given by

$$D_{KL}(P||Q) = \int_{-\infty}^{\infty} p(x) \log \frac{p(x)}{q(x)} dx \quad [3]$$

where  $p$  and  $q$  denote the pdfs of  $P$  and  $Q$ . In the case where  $P$  and  $Q$  are both multivariate Gaussian distributions, the KL divergence can be computed in closed form (1):

$$D_{KL}(P||Q) = \frac{1}{2} \left[ \log \frac{\det \Sigma_q}{\det \Sigma_p} + \text{Tr}(\Sigma_q^{-1} \Sigma_p) - d + (\mu_p - \mu_q)^T \Sigma_q^{-1} (\mu_p - \mu_q) \right] \quad [4]$$

where  $\Sigma_p$  and  $\Sigma_q$  denote the covariance matrices of  $p$  and  $q$ ,  $\mu_p$  and  $\mu_q$  the respective mean vectors, and  $d$  the number of dimensions of the Gaussian. In the case of diagonal Gaussian distributions, Eq.4 reduces to:

$$D_{KL}(P||Q) = \sum_{i=1}^d \left( \log \frac{\sigma_{q,i}}{\sigma_{p,i}} + \frac{\sigma_{p,i}^2 + (\mu_{q,i} - \mu_{p,i})^2}{2\sigma_{q,i}^2} - \frac{1}{2} \right) \quad [5]$$

Even though the KL divergence is not a proper distance metric, as it is not symmetric in its arguments, it can be used to quantify the error of approximation and serve as a metric for comparing different methods.

**Simulation-Based Calibration.** Simulation-based calibration is a recently proposed method for validating the accuracy of posterior samples generated by a Bayesian sampling method (2). It is based on the so called *self-consistency* of the Bayesian joint distribution. Given a sample from the prior distribution  $\tilde{\theta} \sim p(\theta)$  and a sample from the data-generating process  $\tilde{x} \sim p(x|\tilde{\theta})$ , one can integrate  $\tilde{\theta}$  and  $\tilde{x}$  out of the Bayesian joint distribution to recover back the prior of  $\theta$ :

$$p(\theta) = \int p(\theta, \tilde{\theta}, \tilde{x}) d\tilde{x} d\tilde{\theta} \quad [6]$$

$$= \int p(\theta, \tilde{x}|\tilde{\theta}) p(\tilde{\theta}) d\tilde{x} d\tilde{\theta} \quad [7]$$

$$= \int p(\theta|\tilde{x}) p(\tilde{x}|\tilde{\theta}) p(\tilde{\theta}) d\tilde{x} d\tilde{\theta} \quad [8]$$

If the Bayesian sampling method produces samples from the exact posterior, the equality implied by Eq.8 should hold regardless of the particular form of the posterior. Thus, any violation of this equality indicates some error incurred by the sampling method. The authors of (2) propose **Algorithm 1** for visually detecting such violations:

**Algorithm 1** is justified, since Eq.8 implies that the rank statistic defined in line 5 should be uniformly distributed. Hence, any deviations from uniformity indicate some error in the approximate posterior.

---

**Algorithm 1** Simulation-based calibration (SBC) for a single parameter  $\theta$ 

---

- 1: **for**  $i = 1, \dots, n$  **do**
  - 2:   Sample  $\tilde{\theta}^{(i)} \sim p(\theta)$
  - 3:   Simulate a dataset  $\mathbf{x}^{(i)} = q(\tilde{\theta}^{(i)})$
  - 4:   Draw posterior samples  $\{\theta^{(l)}\}_{l=1}^L \sim p(\theta|\mathbf{x}^{(i)})$
  - 5:   Compute rank statistic  $r^{(i)} = \sum_{l=1}^L \mathbb{1}_{[\theta^{(l)} < \tilde{\theta}^{(i)}]}$
  - 6:   Store  $r^{(i)}$
  - 7: **end for**
  - 8: Create a histogram of  $\{r^{(i)}\}_{i=1}^n$  and analyze it for uniformity
-

### 33 Invertible networks

34 Throughout all examples, we use a chain of 10 conditional affine coupling blocks (cACB). Each internal network of  
35 each ACB is implemented as a fully connected neural network with 3 to 4 hidden layers with 64 neurons each. See  
36 <https://github.com/stefanradev93/cINN> for complete implementation details.

### 37 Model details

#### 38 Bayesian regression model.

39 **Summary network.** We use a permutationally invariant neural network as described in (3) for the *i.i.d.* regression data.

#### 40 The Ricker model.

41 **Summary network.** We use a bidirectional long short-term memory (LSTM) recurrent neural network for summarizing the Ricker  
42 time-series into fixed-size vectors.

**Simulation.** We place the following uniform priors over the Ricker model parameters:

$$\rho \sim \mathcal{U}(0, 15) \quad [9]$$

$$r \sim \mathcal{U}(1, 90) \quad [10]$$

$$\sigma \sim \mathcal{U}(0.05, 0.7) \quad [11]$$

43 These ranges are very broad, as datasets generated by extreme parameter values appear implausible in real-world scenarios.  
44 Nevertheless, we stick to broad priors for training, even though parameter recovery might degrade at the extremes. Figure  
45 XXX depicts some Ricker datasets generated by parameters drawn from the specified prior.

#### 46 The Lévy-Flight Model.

47 **Summary network.** We use a permutationally invariant neural network as described in (3) for the *i.i.d.* reaction times (RT) data.

**Simulation.** The following uniform priors over the LFM parameters are used for simulation:

$$v_0 \sim \mathcal{U}(0, 6) \quad [12]$$

$$v_1 \sim \mathcal{U}(-6, 0) \quad [13]$$

$$zr \sim \mathcal{U}(0.3, 0.7) \quad [14]$$

$$a \sim \mathcal{U}(0.6, 3) \quad [15]$$

$$t_0 \sim \mathcal{U}(0.3, 1) \quad [16]$$

$$\alpha \sim \mathcal{U}(1, 2) \quad [17]$$

48 These priors are broad enough to cover the range of realistic reaction times observed in choice RT experiments.

#### 49 The stochastic SIR model.

50 **Summary network.** We use a 1D convolutional neural network for summarizing the SIR time-series into fixed-size vectors.

**Simulation.** We place the following uniform priors over the two rate parameters of the stochastic SIR model:

$$\beta \sim \mathcal{U}(0.01, 1) \quad [18]$$

$$\gamma \sim \mathcal{U}(0.01, \beta) \quad [19]$$

51 Figure XXX depicts some SIR datasets generated by parameters drawn from the specified priors.

#### 52 Single-Cell RNA Sequencing.

53 **Summary network.** We use two permutationally invariant networks as described in (3) for embedding the count matrices generated  
54 with the *Splat* simulator (4). The first network goes over the cells and the second over the genes axis of the count matrices.

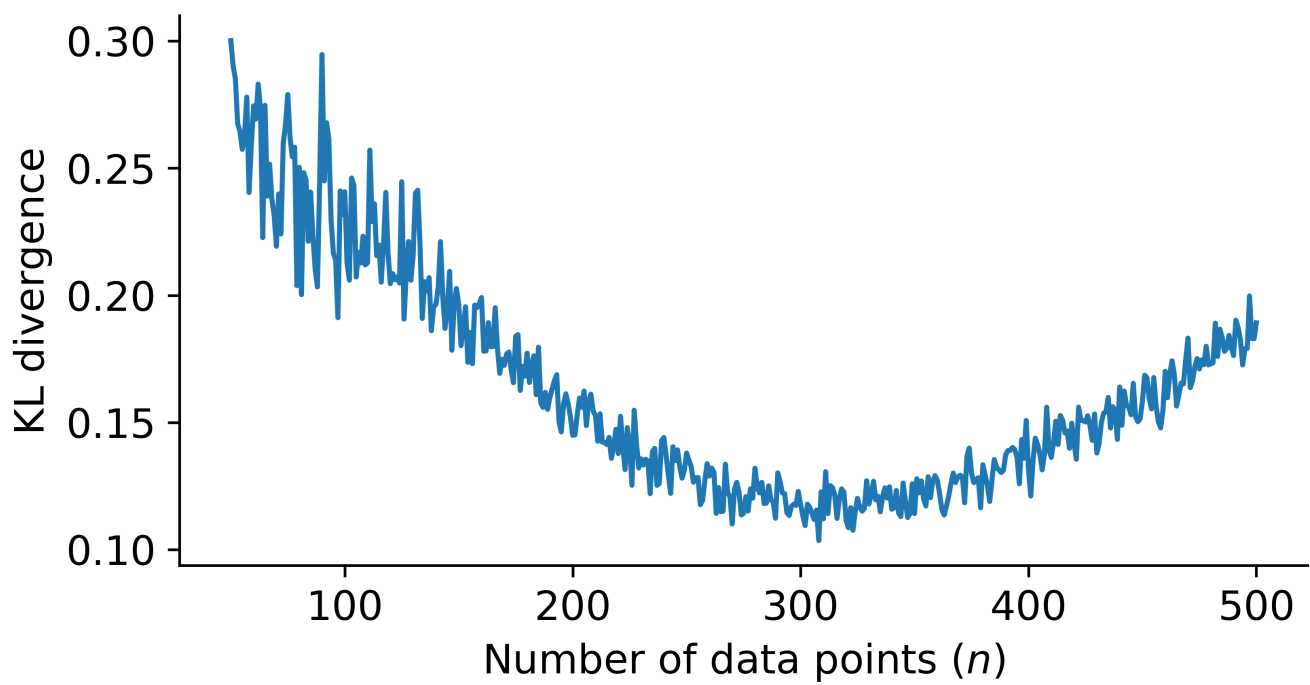


Fig. S1. Second figure

**Simulation.** We place the following uniform priors over the parameters of the *Splat* simulation:

$$\alpha \sim \mathcal{U}(1, 2) \quad [20]$$

$$\beta \sim \mathcal{U}(0.1, 5) \quad [21]$$

$$\mu^L \sim \mathcal{U}(6, 10) \quad [22]$$

$$\sigma^L \sim \mathcal{U}(1, 2) \quad [23]$$

$$\pi^O \sim \mathcal{U}(0.01, 0.5) \quad [24]$$

$$\mu^O \sim \mathcal{U}(0.5, 5) \quad [25]$$

$$\sigma^O \sim \mathcal{U}(0.1, 2) \quad [26]$$

$$\phi \sim \mathcal{U}(0.1, 0.9) \quad [27]$$

Movie S1. Type caption for the movie here.

Movie S2. Type caption for the other movie here. Adding longer text to show what happens, to decide on alignment and/or indentations.

Movie S3. A third movie, just for kicks.

Additional data table S1 (**dataset\_one.txt**)

Type or paste caption here.

Additional data table S2 (**dataset\_two.txt**)

Type or paste caption here. Adding longer text to show what happens, to decide on alignment and/or indentations for multi-line or paragraph captions.

## References

1. Hershey JR, Olsen PA (2007) Approximating the kullback leibler divergence between gaussian mixture models in 2007 *IEEE International Conference on Acoustics, Speech and Signal Processing-ICASSP'07*. (IEEE), Vol. 4, pp. IV–317.
2. Talts S, Betancourt M, Simpson D, Vehtari A, Gelman A (2018) Validating bayesian inference algorithms with simulation-based calibration. *arXiv preprint arXiv:1804.06788*.
3. Bloem-Reddy B, Teh YW (2019) Probabilistic symmetry and invariant neural networks. *arXiv preprint arXiv:1901.06082*.
4. Zappia L, Phipson B, Oshlack A (2017) Splatter: simulation of single-cell rna sequencing data. *Genome biology* 18(1):174.